Comparative of ballistocardiogram processing methods based on fiber specklegram sensors

Luis Reyes-González, Luis Rodríguez-Cobo, and José-Miguel López-Higuera,

***Abstract*— The ballistocardiogram is a graphic representation of the movements of the body associated with cardiac activity. In this paper, a ten minutes ballistocardiogram have been captured for ten different volunteers with a polymer optical fiber (POF) specklegram sensor. This transducer, which is composed by a CCD camera, a laser emitting diode and two meters of POF, allows to capture the ballistocardiogram by analyzing how the induced speckle pattern changes over the time. These changes are related to cardiac activity. Several processing methods have been compared to determine which method achieve the best performance: Complex Cepstrum, Power of Spectral Density (PSD), Pam-Tompkins algorithm, Wavelet, Autocorrelation, Savitzky-Golay filter, Mean Absolute Deviation and Hilbert transform. Accuracy and resources consumption have been characterized and compared for these methods. Hilbert, PSD and Savitzky-golay exhibit both small error and computational cost. This paper describes a baseline for main frequency determination of POF-based ballistocardiogram signals in real time.**

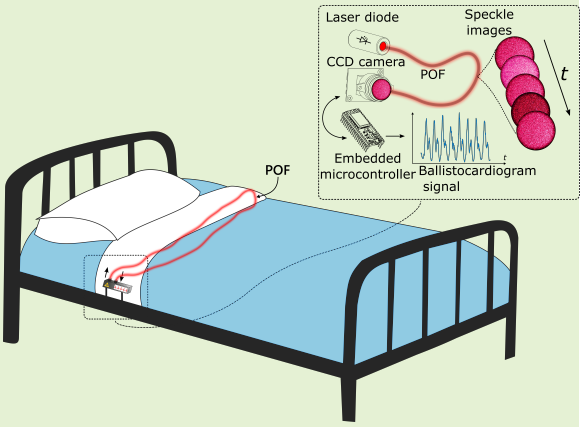

***Index Terms*— Ballistocardiogram (BCG), Fiber-optic sensors, noninvasive physiologic monitoring, sensor data processing, Speckle.**

I. Introduction

SINCE early 1940s, the interest in pulse monitoring has suited crescent interest. It contributes to different benefits to the patient, as reported in [1] [33]. The main technique reported in the bibliography is the electrectrocardiogram (ECG) however, during last years, the reported works were focused on monitoring pulse without direct contact, improving the comfort for the patients. In this area is where ballistogram (BCG) becomes more important.

The ballistocardiogram is a graphic representation of the movements of the body imparted by ballistic forces (recoil and impact) associated with cardiac contraction and ejection of blood and with the deceleration of blood flow through the large blood vessels. These represented movements are periodical and can be quantified periodically, which results on the pulse [4]. For its own definition, BCG signal is deeply influenced by movements, which are the main source of noise.

An example of different type of signals used for pulse monitoring are illustrated in Figure 1. It should be noticed that signal noise ratio (SNR) in ECG signal is better than in BCG signal because the main peak is higher and the noise peak are shorter, respectively. But, at the end, the pulse monitoring is reduced to the frequency of the main peaks in each signal, R in ECG and J in BCG [13], [4]. Although these peaks corresponds to different states of the heartbeat, the period between them corresponds to heart rate.

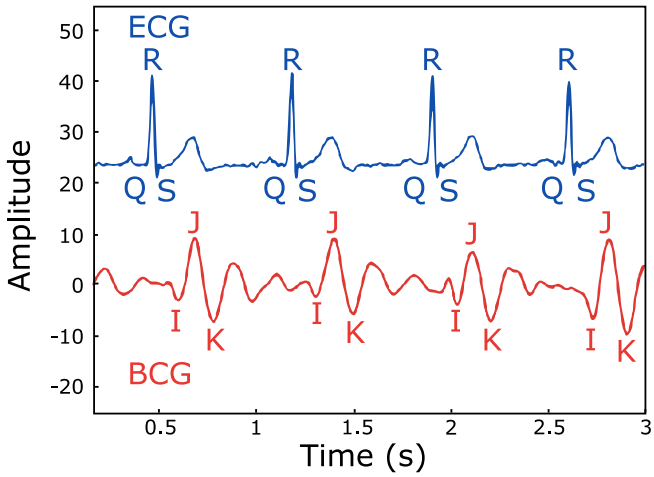

Fig. 1. Representation of typical electrocardiogram (ECG) and ballistocardiogram (BCG) signals with the names of the different peaks of interest attached.

The ballistocardiogram signal is captured by a transducer,

This work has been co-supported by the project PID2019-107270RB-C21 funded by MCIN/ 432 AEI /10.13039/501100011033.

Luis Reyes-González is with the Instituto de Investigación Sanitaria Valdecilla (IDIVAL), Cantabria, Spain (e-mail: reyeslr@unican.es).

Luis Rodríguez-Cobo, is with the CIBER-BBN, Instituto de Salud Carlos III, Madrid, Spain

José-Miguel López-Higuera is with the Photonics Engineering Group, University of Cantabria, 39005 Santander, Spain, with the Instituto de Investigación Sanitaria Valdecilla (IDIVAL), Cantabria, Spain and with the CIBER-BBN, Instituto de Salud Carlos III, Madrid, Spain.

which transforms the movements of the body into a measurable signal. There are several kind of transducers that can be employed, electromechanical, pneumatic, piezolectric, etc. Optical transducers are becoming more important, specially Fiber Specklegram Sensors, because of this a polymer optical fiber (POF) has been employed as transducer. Several examples have been reported in literature as [19], [9], [21], [17], [32], [8], [31], [12].

II. Speckle Interferometry and Ballistocardiogram

Based on speckle interferometry, a relatively simple experimental setup (Figure 2) can be employed to detect extremely small mechanical perturbations provoked to a multimode fiber, exhibiting an extremely high sensitivity at a reduced cost. The main advantages of this kind of sensors is its low cost and electromagnetic field immunity. This allows to capture a precise ballistocardiogram, hence pulse monitoring of patient, in situations where electronic is not an option because of electromagnetic field (Nuclear magnetic resonance situations for example).

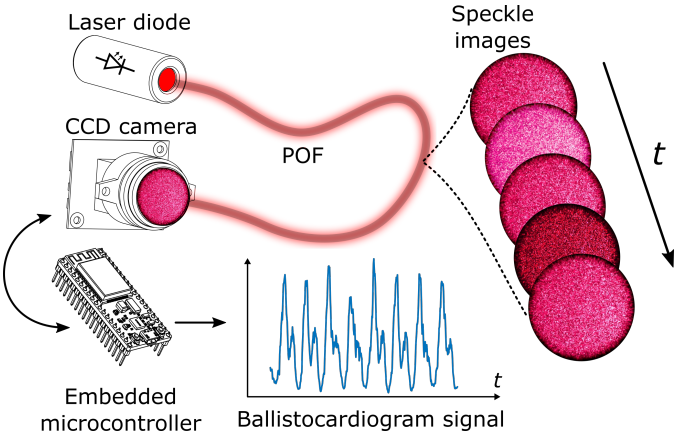

Fig. 2. Schema of the POF based specklegram system employed to capture the ballistocardiogram signal.

Speckle interferometry in a multimode optical fiber is caused by the different phase velocities of each propagation mode. These propagation conditions create an unique interference pattern at the end of the fiber due to the phase delay between modes thus, consequently, any variation of the propagation conditions will provoke differences into the final speckle pattern [20].

The speckle pattern launched at the fiber output is the result of the sum of the contributions of all propagated modes. Depending on the laser and fiber properties the interference pattern exhibits enough contrast to be analyzed with a commercial low cost CCD camera. Despite of a possible variation of the intensity of each individual speckle, the total intensity of the pattern should remain constant [26]. The number of modes, M, which are given by Equation (1), determines the number of speckle.

$$M = \frac{V^2}{2} \quad \text{with} \quad V = \frac{2a\pi}{\lambda}\sqrt{n_{co}^2 - n_{cl}^2} \tag{1}$$

where a is the core radius, λ is the wavelength of the laser, and n_{co} and n_{cl} are the refractive indexes of core and cladding, respectively [29].

Any external perturbation applied to the optical fiber affects the propagation conditions of the fiber and, therefore, to the speckle pattern. The pattern can be acquired at the end of the fiber by a CCD camera as a temporal sequence. A relationship between the speckle pattern variation and the measured external perturbation can be related. According to the model [26], perturbation affects both the propagation and the interference pattern, *F(t)*, which is related to the intensity of each speckle, I_i. As shown in Equation (2), the intensity of each speckle can be calculated as the integration of the spatial intensity function for each speckle area.

$$I_i = Ai + \{1 + B_i \times [cos(\delta_i) - F(t) \cdot \phi_i \times sin(\delta_i\} \tag{2}$$

In this equation, A_i represents the self-mode interaction, and *F(t)*, B_i, and ϕ_i define the interaction between modes. *F(t)* is the external perturbation applied to the fiber. The argument of the harmonic functions δ_i describes the difference in propagation constant and the random phase of all the pairs of modes considered within the same speckle intensity. A_i, B_i, ϕ_i and δ_i are constant values for any given i.

A differential processing is applied to Equation (2) in order to extract the information *F(t)*. The sum of the absolute value of the changes in all the signals is computed as (ΔI_t) based on the pixel sensitivity (c) and described by:

$$\Delta I_T = C \cdot \frac{dF(t)}{dt} = C \cdot \Delta F \tag{3}$$

A differential processing method is applied to calculate the relation between the speckle pattern variation and the external perturbation measured (ΔI_D) for every i'th pixel:

$$\Delta I_D\{i\} = \frac{1}{K \cdot MN} \sum_{n=0}^{N-1} \sum_{n=0}^{M-1} \left| I_{nm}^{i-1} - I_{nm}^{i} \right| \tag{4}$$

where K is the full scale value of the speckle pattern color map (for example, $K = 255$ for 8 bits grayscale system) and I_{mn} corresponds to the pixel of the n, m (considering a speckle pattern of N x M pixels adquired for the CCD device) position of the i'th speckle pattern. The relation described by Equation (4) assumes that the total intensity of the speckle pattern remains constant under perturbations. The obtained value quantifies the power migration between individual speckles within the pattern.

This method provides a way to measure dynamic changes in fiber perturbations limited by the CCD sampling rate. The sensitivity of this fiber specklegram sensor (C in Eq. (3)) is mainly given by the amount and contrast of the speckles comprised within the captured images and can be determined by a proper tuning of the coherent source, multimode fiber and detector.

Based on this relatively simple setup, a fiber specklegram sensor is able to capture the dynamic changes of the body during a heartbeat. When a POF is in mechanical contact to the body of the patient, the heartbeat provokes changes

in the specklegram with the same frequency as the pulse. Therefore, the pulse monitoring problem can be reduced to detect the frequency of J-peaks in a ballistocardiogram signal captured with a POF based sensor. An example of captured ballistocardiogram compared to a gold standard pulse signal is depicted in Figure 3. It can be noticed that the captured J peaks are in a very good agreement with the reference. Each pulse peak is marked for an easy visualization.

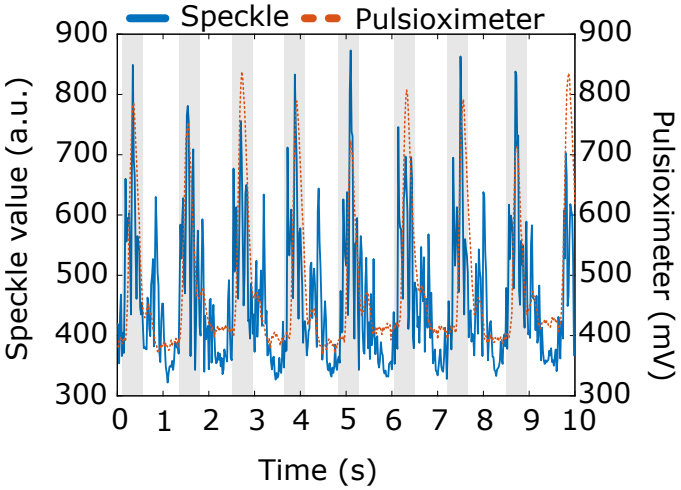

Fig. 3. Representation of captured ballistocardiogram and gold standard reference (pulseoximeter) signals with pulse peaks marked.

III. Experimental setup

The ballistocardiogram signals of 10 different volunteers have been captured to probe which method exhibit the best performance. They are 9 males and 1 female, with an age average of 30 years and standard deviation of $3,4$ years. All the captured signals have an approximate duration of 10 minutes. For validation purpose, at the same time, the pulse was monitored with a pulseoximeter [10] as gold standard reference.

A. Ballistocardiogram acquiring signal system

The capture device is a polymer optical fiber (POF) based one. This consist in 2 meters of POF with a core diameter of 240 μm, a semiconductor laser diode emitting at 638 nm and a CCD camera (OV2640) which is able to maintain a 50 frames per second (FPS) rate.The selected POF model is $SK-10$ from Mitsubishi Chemical Corporation. The core material of the POF is made of Polymethyl-Methacrylate Resin with a refractive index of 1.49 and its cladding material is Fluorinated Polymer. The data acquisition is performed by an embed microcontroller, which handles the camera and process the data from it due to obtain the ballistocardiogram signal. The optical fiber is placed on the mattress under patient's low back, as [21] has proved as best placement, capturing ballistocardiogram signal across it. The acquisition system and its placement are illustrated in Figure 4.

Before analyzing the performance of different processing methods, a pre-processing step is applied to the ballistocardiogram signals. Each signal has been normalized by subtracting the mean to the original to suppress the baseline component. This normalization highlights the peaks of the desired heartbeat frequencies. After the normalization, the signal have been windowed in a 30 seconds moving window, with increments of one second. This means an overlap of 29 seconds and an effective frequency of 60 pulses per minute once the window is fulfilled.

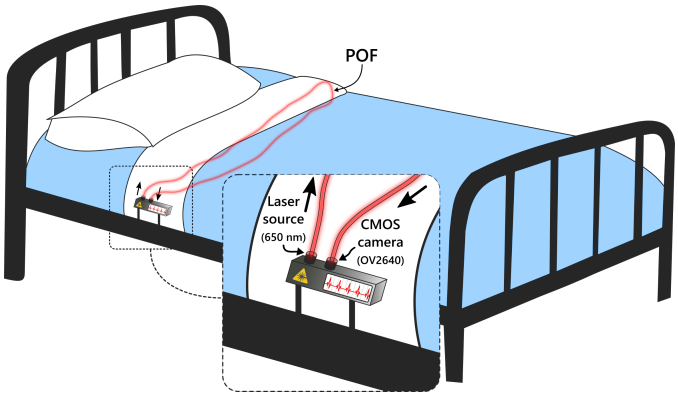

Fig. 4. Scheme of ballistocardiogram acquiring signal system.

The different processing methods evaluated in this paper are applied for each window in time. These methods are the following:

- The Complex Cepstrum.
- Power of Spectral Density.
- Pan-Tompkins algorithm.
- Wavelet.
- Autocorrelation.
- Savitzky-Golay filter.
- Mean Absolute Deviation.
- Hilbert transform.

These methods have been selected according to 2 different criteria: they are widely used in bibliography to obtain pulse from BCG signal or they are used to obtain frequency of a signal which is similar enough to the captured ballistocardiograms. Different methods are included even when the achieved results are not the expected because the aim of this paper is to find the best base method to evaluate pulse from ballistocardiogram. But, also more complex analysis could be done by applying the information provided from the rest of the methods or others not included in this comparative.

The aim of the paper is to obtain the pulse rate from ballistocardiogram with different signal processing methods, so it is mandatory to use a reference method for pulse. In this case, a finger pulseoximeter has been used as gold standard [10]. The captured signal is windowed in a 30 seconds window, same size as speckle windows.Then, FFT is applied for each segment and maximum peak detected as heart rate. The error is characterized in each window, for each processing method according to Equation (5).

$$Error = |Value_{control} - Value_{speckle}| \tag{5}$$

B. The Complex Cepstrum

The complex cepstrum is a method for obtaining periodical information from frequency spectra. It is widely used in mechanical frequency analysis [18] and brain waves analysis [16]. Formally, the complex cepstrum of a data sequence is the inverse z-transform of the complex logarithm of the z-transform of the data sequence [2]:

$$\widehat{x}(nT) = \frac{1}{2\pi j}\oint_c log(X(z))z^{n-1}dz \tag{6}$$

where $\widehat{x}(0) = log[x(0)]$ and $X(z)$ is the z-transform of the data sequence $x(nT)$. Heart rate is estimated collating the cepstrum peak detected within each window of cepstrogram. The time lag values of the peaks are used in calculating heart rate [34].

C. Power of Spectral Density

Power of Spectral Density (PSD) is a normalization of the FFT magnitude by frequency, so the high frequencies are attenuated [7]. This benefit can be exploited for hearth rate monitoring due to the low frequencies of the signal (from the order of 0.8 to 2 Hz). By definition, PSD describes how power of a signal is distributed over frequency [28]. According to the Parseval's theorem [5], PSD is defined in (7):

$$S_{xx}(f) = \lim_{T\to\infty}\frac{1}{T}|\widehat{x}_T(f)^2| \tag{7}$$

D. Pan-Tompkins algorithm

Pan-Tompkins algorithm is commonly used to detect heart rate from electrocardiogram signal (ECG). Although, ballistocardiogram and electrocardiogram signals are different but, assuming the correlation between J and K peaks, as showed in Figure 3, it is interesting to test Pan-Tompkins algorithm. First of all, a band pass filter is applied to the signal, followed by differentiation of signal and squaring it. Finally, a moving window integration is done. Once the peaks are maximized with Pan-Tompkins algorithm [15], FFT is applied to resultant signal in order to detect heart rate.

E. Wavelet

Wavelet analysis is the decomposition of a signal in a small waves (wavelets) with different frequencies. It is becoming more important in signal analysis because its time-localized and frequency-localized behavior [25] and also because its denoising property [11]. After testing all small waves, symlet 4 has been chosen due to it was the one with the best performance. Simlet 4 is near symmetric, orthogonal and biorthogonal . The wavelet function and the scaling function can be checked in figure 5.

F. Autocorrelation

Autocorrelation is the correlation of a signal with a delayed copy of itself. The periodicity of the signal is then marked by the peaks of the autocorrelation, which in this scenario represents the delay between J peaks. The autocorrelation

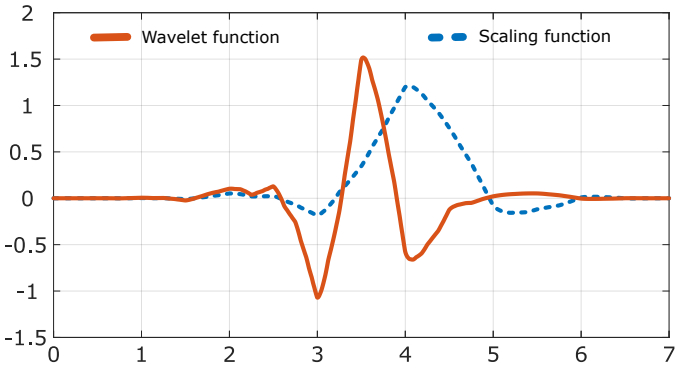

Fig. 5. Graphic representation of Symlet 4 wavelet (solid line) and its scaling function (dotted line).

signal exhibits two different periods, breathing and heart rate, that correspond with the different peaks of the signal, so a threshold is required. In order to minimize noise, all the peaks over the threshold, that correspond to the heart rate, are located in the window. Finally, the heart rate obtained is the mean of the time difference between all heart beats [14], [24]. Because analysis window is 30 seconds, the delay for autocorrelation is 30 seconds too.

G. Savitzky-Golay filter

Savitzky-Golay filter was first pubilished in 1964 [22] [27]. It is a digital filter which function is to smooth data, this is done by polynomial regression. One of the mayor advantage of this method is that it preserves the width and the peaks in the signal waveform [23], this is the reason that can be useful for ballistocardiogram signals.

H. Mean Absolute Deviation

The mean absolute deviation is a moving dispersion technique [3], which applied to the ballistocardiogram signal removes low frequency components as breathing. Mean absolute deviation is implemented in each window, as showed in Equation 8:

$$g(i) = |spk(i) - mean(spk)| \tag{8}$$

where $spk(i)$ is the ballistocardiogram value in i instant of time and $mean(spk)$ the mean of the current window. The mean of the current window is employed because, in real time, it can not be determined the mean all over the time.

I. Hilbert transform

Hilbert transform method is used due to one of the main properties of the Hilbert Transform, when a Fast Fourier Transform is applied to the signal $g(t)$, the Hilbert transform does not change the magnitude of $G(f)$, it changes only the phase. So if it applies to the ballistocardiogram signal, it allows to filter and reconstruct it without altering the magnitude of the FFT peaks.

Formally, the Hilbert transform is the response to $g(t)$ of a linear time-invariant filter having impulse response $1/\pi t$, this

filter is called Hilbert Transformer, which is the convolution of $g(t)$ with the signal $1/\pi t$. The Equation 9 express the definition of the Hilbert Transform [30], [6].

$$\mathcal{H}[g(t)] = \frac{1}{\pi}\int_{-\infty}^{\infty}\frac{g(t-\tau}{\tau})d\tau \tag{9}$$

IV. Results and discussion

Different metrics have been measured in order to characterize accuracy and efficiency of each method. Understanding accuracy as the difference between the obtained value from ballistocardiogram with each method and the heart rate determined by gold standard, in our case pulseoximeter. The accuracy has been evaluated with three different metrics: the averaged error of all the volunteers for each instant and method; and the mean and standard deviation of the previous values.

According to Figure 6, it can be noticed that some methods exhibit high absolute error values, which means worse accuracy: Cepstrum, Autocorrelation and Mean Absolute Deviation. Based on these results, it should be noticed that the BCG signal is different for each person and the breathing component is an important part of the signal. This means different amplitudes of J peaks and breathing components for each person, that difficults the autodetection of pulse peaks. This is one of the main reasons of the poor accuracy of autocorrelation method, and for it, autocorrelation rarely is applied as unique analysis method in bibliography [14] [24]. Another important characteristic of BCG signal is its low frequency, the relevant frequencies are between 0.8 and 2 Hz. Due to the low frequency of the interest signals, cepstrum method exhibits a low accuracy. This is mainly provoked by the applied logarithmic conversion that difficults the detection of the fundamental frequency, because they are very close frequencies.

The other method with low accuracy is the absolute value of the mobile mean, because it can not be implemented in real time because the absolute mean value can not be determined a-priori in a real-time configuration, thus the mean value of each window is taken instead. This implies that all the signal is not referenced to the same value, so this induces error in heart rate detection.

Pam-Tompkins method exhibits a high error when processing BGC signals, but not as large as the error of the methods commented before. Due to its typical application, ECG signals, it is important to compare both type of signal to explain this accuracy difference. They both have prominent peaks, R and J, and smaller peaks, Q and S in ECG and I and K in BCG. Refer to Figure 1 for more information about the signals. But, the main difference is the amplitude of all of these peaks, the smalls ones in BCG are higher than in ECG and the prominent ones in BCG are smaller than in ECG. This results on a worse SNR value for BCG signal. So, the low accuracy of the Pam-Thompkins method is because of the difference between the SNR values of BCG and ECG signals.

On the other hand, the methods that exhibit better accuracy are: Hilbert, PSD, Wavelet and Savitzky-Golay. The error of these methods is always under 10 BPM, with lower errors for

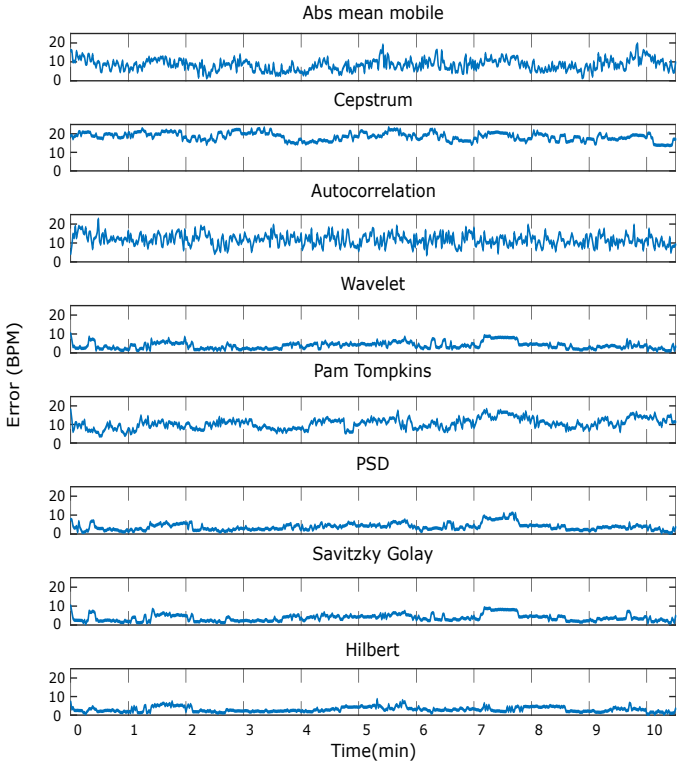

Fig. 6. Absolute error of different processing methods versus time. The **10** minutes represented are the mean error of each method for all volunteers in each instant of time.

almost all the time. In order to distinguish the best method in terms of accuracy, the stadistic error with mean and standard deviation are depicted in Figure 7. Cepstrum, Pam-Tompkins, Autocorrelation and Absolute value of Mean Mobile have the largest mean error (smallest accuracy), as expected. Anyway, considering a mean pulse heart rate of 70 BPM, the error is around the 20% for all these methods, which fix into the range of the bibliography [24]. The standard deviation is approximately the 30% of the mean for these methods, it is important because this confirm the hypothesis of the main problem of these methods, the breathing interference.

Focusing on the methods with the best accuracy: PSD, Wavelet, Hilbert and Savitzky-Golay. All of them have a mean error under the 5% of the typical heart rate of 70 BPM, with an standard deviation under the half of the mean. These values denote that PSD, Wavelet, Svitzky-Golay and Hilbert transform have a remarkable accuracy and they are suitable to use in a commercial device to monitor pulse rate.

Based on Figure 7, there are not relevant differences between the processing methods which achieve the best accuracy, so the efficiency has been quantified, understanding it as the maximum accuracy with minimal processing cost. Because at this point the accuracy is well characterized due to the depicted Figures, the efficiency is closely related to the computational cost so, in order to establish a baseline of real time analysis, it has been evaluated for each method. The processing has been performed in a computer with 16 Gb of RAM DDR4 and CPU $i5-8500$ with the software Matlab®R2021b. The mean of the computing time of 10 minutes windows for all methods

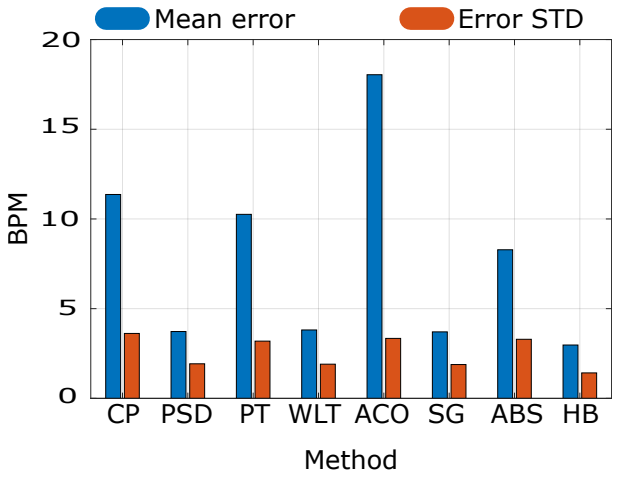

Fig. 7. Arithmetic mean and standard deviation of error for each processing method. These values are calculated from all volunteers over all the time. The methods names in X axis, ordered from left to right, correspond with: Cepstrum, PSD, Pam-Tompkins, Wavelet, Autocorrelation, Savitzky-Golay, ABS mobile mean and Hilbert transform.

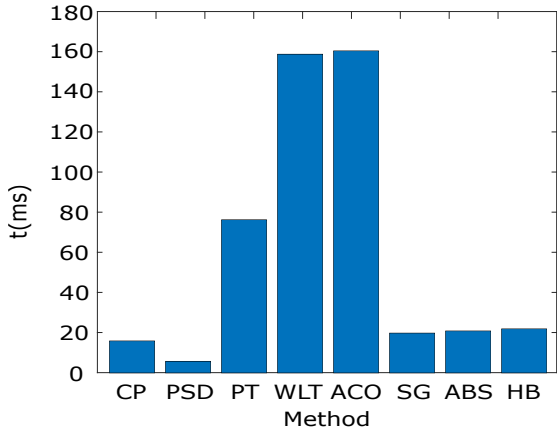

Fig. 8. Processing time for each processing method. The represented time is the mean of the processing time for all volunteers in each method. The methods names in X axis, ordered from left to right, correspond with: Cepstrum, PSD, Pam-Tompkins, Wavelet, Autocorrelation, Savitzky-Golay, ABS mobile mean and Hilbert transform.

are compared in Figure 8. Lower accuracy methods have been also included in this comparison, because it would be useful for different signals or processings to have a reference of the computing time of these methods. According to Figure 8, and focused on the best accuracy methods, Hilbert, PSD, Wavelet and Savitzky-Golay, there are relevant differences between their processing cost. PSD is the fastest one, this is because of the Parseval's definition, as reported in Equation 7, which normalized the energy of the FFT of the signal. According to the previous definitions, the faster methods are all based on a decomposition of the signal in different mother wavelets (Simlet 4 for wavelet transform and $e^{-2\pi it}$ for FFT), it was expected that the simplest one would be the fastest, which is PSD. Next methods with low computational cost, Savitzky-Golay and Hilbert transform, have no remarkable difference of processing time between them. Although their processing time is short enough for real time, 10 minutes are processed in 20 ms, they spend 4 times more than PSD. Finally, the wavelet method needs 32 times the PSD time, but, 160 ms for 10 minute processing keeps this method suitable for real time processing.

The benefits and drawbacks of the different processing methods are detailed in Table IV.

It is mandatory to evaluate pulse monitoring in real time, but, different accuracies would be accepted depending on the context. Besides, only simple methods have been considered in this paper, but, their accuracy can be improved by combing them, and pre or post-processing the ballistocardiogram signal or the obtained pulse.

Method	Benefits	Drawback
Cepstrum	Low computational cost	Armonic detection Precision with low frequency signals
PSD	Lowest comp. cost Normalization reduces armonic peaks	Better perfomance with longer time windows
Pam-Tompkins	Not suitable for BCG	High computational Cost Low perfomance
Wavelet	Reduces the necesary filters by aproximatting to wavelet Accurate	High computational cost
Autocorrelation	Not suitable for BCG	Low accuracy High interferences with armonics
Savitzky-Golay	Low computational cost	It suposes no significant difference
Abs mean mobile	Low computational cost By definition, supress the DC component	Unable to implement in real time with short windows
Hilbert	Low computational cost Filter noise by altering phase in FFT	Phase shift

TABLE I
BENEFITS AND DRAWBACKS FOR EACH METHOD

V. Conclusion

This paper settles a baseline to start a real time processing of ballistocardiogram signals. In this purpose, a comparative between different methods for processing ballistocardiogram signals of the literature have been performed. The comparative has been focused on processing error and processing cost. It is important to consider both for real time and cost purposes. The processing error has been characterized with the stadistic of mean and standard deviation of pulse error.

According to previous works [21] [19], this one explores new processing methods that achieve better accuracy with a low computational cost. The processing methods: Hilbert, PSD, and Savitzky-Golay, achieve really good metrics in both fields, accuracy and computational cost. It would be necessary to take into account each one of them according to the application. This would specify the compromise between precision and the available resources for the processing, and this paper will allow to select the best method for each situation.

References

[1] Wendy Chaboyer, Lukman Thalib, Michelle Foster, Carol Ball, and Brent Richards. Predictors of adverse events in patients after discharge from the intensive care unit. *American Journal of Critical Care*, 17(3):255–263, may 2008.

[2] D.G. Childers, D.P. Skinner, and R.C. Kemerait. The cepstrum: A guide to processing. *Proceedings of the IEEE*, 65(10):1428–1443, 1977.

[3] Sun-Taag Choe and We-Duke Cho. Simplified real-time heartbeat detection in ballistocardiography using a dispersion-maximum method. *Biomedical Research-tokyo*, 28:3974–3985, 2017.

[4] Richard S Gubner, Manuel Rodstein, and Harry E Ungerleider. Ballistocardiography: An appraisal of technic, physiologic principles, and clinical value. *Circulation*, 7(2):268–286, 1953.

[5] S. S. Kelkar, L. L. Grigsby, and J. Langsner. An extension of parseval's theorem and its use in calculating transient energy in the frequency domain. *IEEE Transactions on Industrial Electronics*, IE-30(1):42–45, 1983.

[6] Frank R Kschischang. The hilbert transform. *University of Toronto*, 83:277, 2006.

[7] P. Laguna, G.B. Moody, and R.G. Mark. Power spectral density of unevenly sampled data by least-square analysis: performance and application to heart rate signals. *IEEE Transactions on Biomedical Engineering*, 45(6):698–715, jun 1998.

[8] Arnaldo G. Leal-Junior, Anselmo Frizera, Carlos Marques, and Maria Jose Pontes. Optical fiber specklegram sensors for mechanical measurements: A review. *IEEE Sensors Journal*, 20(2):569–576, jan 2020.

[9] M. Lomer, L. Rodriguez-Cobo, P. Revilla, G. Herrero, F. Madruga, and J. M. Lopez-Higuera. Speckle POF sensor for detecting vital signs of patients. In José M. López-Higuera, Julian D. C. Jones, Manuel López-Amo, and José L. Santos, editors, *SPIE Proceedings*. SPIE, jun 2014.

[10] Marta Elena Losa-Iglesias, Ricardo Becerro de Bengoa-Vallejo, and Klark Ricardo Becerro de Bengoa-Losa. Reliability and concurrent validity of a peripheral pulse oximeter and health–app system for the quantification of heart rate in healthy adults. *Health Informatics Journal*, 22(2):151–159, jul 2014.

[11] Sheila R Messer, John Agzarian, and Derek Abbott. Optimal wavelet denoising for phonocardiograms. *Microelectronics Journal*, 32(12):931–941, dec 2001.

[12] Rui Min, Xuehao Hu, Luis Pereira, M. Simone Soares, Luís C.B. Silva, Guoqing Wang, Luis Martins, Hang Qu, Paulo Antunes, Carlos Marques, and Xiaoli Li. Polymer optical fiber for monitoring human physiological and body function: A comprehensive review on mechanisms, materials, and applications. *Optics &amp Laser Technology*, 147:107626, mar 2022.

[13] David M Mirvis and Ary L Goldberger. Electrocardiography. *Heart disease*, 1:82–128, 2001.

[14] M. Nakano, T. Konishi, S. Izumi, H. Kawaguchi, and M. Yoshimoto. Instantaneous heart rate detection using short-time autocorrelation for wearable healthcare systems. In *2012 Annual International Conference of the IEEE Engineering in Medicine and Biology Society*. IEEE, aug 2012.

[15] Jiapu Pan and Willis J. Tompkins. A real-time QRS detection algorithm. *IEEE Transactions on Biomedical Engineering*, BME-32(3):230–236, mar 1985.

[16] S. Pazhanirajan and P. Dhanalakshmi. EEG signal classification using linear predictive cepstral coefficient features. *International Journal of Computer Applications*, 73(1):28–31, jul 2013.

[17] Peter Podbreznik, Denis Donlagic, Dejan Lesnik, Boris Cigale, and Damjan Zazula. Cost-efficient speckle interferometry with plastic optical fiber for unobtrusive monitoring of human vital signs. *Journal of Biomedical Optics*, 18(10):107001, oct 2013.

[18] Robert Bond Randall and RANDALL RB. Cepstrum analysis and gearbox fault diagnosis. 1976.

[19] Luis Rodriguez-Cobo, Mauro Lomer, Adolfo Cobo, and Jose-Miguel Lopez-Higuera. Optical fiber strain sensor with extended dynamic range based on specklegrams. *Sensors and Actuators A: Physical*, 203:341–345, dec 2013.

[20] Luis Rodriguez-Cobo, Mauro Lomer, Carlos Galindez, and J. M. Lopez-Higuera. Speckle characterization in multimode fibers for sensing applications. In Ángel F. Doval and Cristina Trillo, editors, *SPIE Proceedings*. SPIE, sep 2012.

[21] Alberto Rodríguez-Cuevas, Eusebio Real Peña, Luis Rodríguez-Cobo, Mauro Lomer, and José Miguel López Higuera. Low-cost fiber specklegram sensor for noncontact continuous patient monitoring. *Journal of Biomedical Optics*, 22(3):037001, mar 2017.

[22] Abraham. Savitzky and M. J. E. Golay. Smoothing and differentiation of data by simplified least squares procedures. *Analytical Chemistry*, 36(8):1627–1639, jul 1964.

[23] Ronald Schafer. What is a savitzky-golay filter? [lecture notes]. *IEEE Signal Processing Magazine*, 28(4):111–117, jul 2011.

[24] Masatoshi Sekine and Kurato Maeno. Non-contact heart rate detection using periodic variation in doppler frequency. In *2011 IEEE Sensors Applications Symposium*. IEEE, feb 2011.

[25] M Sifuzzaman, M Rafiq Islam, and MZ Ali. Application of wavelet transform and its advantages compared to fourier transform. *Journal of Physical Sciences*, 2009.

[26] W. B. Spillman, B. R. Kline, L. B. Maurice, and P. L Fuhr. Statistical-mode sensor for fiber optic vibration sensing uses. *Applied Optics*, 28(15):3166, aug 1989.

[27] Jean. Steinier, Yves. Termonia, and Jules. Deltour. Smoothing and differentiation of data by simplified least square procedure. *Analytical Chemistry*, 44(11):1906–1909, sep 1972.

[28] Petre Stoica, Randolph L Moses, et al. *Spectral analysis of signals*. Pearson Prentice Hall Upper Saddle River, NJ, 2005.

[29] Jernej Škrabec, Boris Cigalec, Dejan Lešnik, Denis Donlagić, and Damjan Zazula. Preliminary detection of periodic perturbations using speckle imaging and interframe gradient. In *Proceedings of the 11th WSEAS International Conference on Applied Informatics and Communications, and Proceedings of the 4th WSEAS International Conference on Biomedical Electronics and Biomedical Informatics, and Proceedings of the International Conference on Computational Engineering in Systems Applications*, AIASABEBI'11, page 251–256, Stevens Point, Wisconsin, USA, 2011. World Scientific and Engineering Academy and Society (WSEAS).

[30] Qingsong Xie, Guoxing Wang, and Yong Lian. Heart rate estimation from ballistocardiography based on hilbert transform and phase vocoder. In *2018 IEEE Asia Pacific Conference on Circuits and Systems (APCCAS)*. IEEE, oct 2018.

[31] Kaikai Xu. Silicon electro-optic micro-modulator fabricated in standard CMOS technology as components for all silicon monolithic integrated optoelectronic systems $\sup*/sup.Journalof Micromechanicsand Microengineering, 31(5) : 054001, apr2021$.

[32] Kaikai Xu, Yanxu Chen, Timothy A. Okhai, and Lukas W. Snyman. Micro optical sensors based on avalanching silicon light-emitting devices monolithically integrated on chips. *Optical Materials Express*, 9(10):3985, sep 2019.

[33] Michael P Young, Valerie J Gooder, Karen McBride, Brent James, and Elliott S Fisher. Inpatient transfers to the intensive care unit. *Journal of general internal medicine*, 18(2):77–83, 2003.

[34] Yongwei Zhu, Victor Foo Siang Fook, Emily Hao Jianzhong, Jayachandran Maniyeri, Cuntai Guan, Haihong Zhang, Eugene Phua Jiliang, and Jit Biswas. Heart rate estimation from FBG sensors using cepstrum analysis and sensor fusion. In *2014 36th Annual International Conference of the IEEE Engineering in Medicine and Biology Society*. IEEE, aug 2014.